

## Supporting Information

### Blocking Polymerization of CTFs Induces Plentiful Structural Terminations for Synchronous Removal of Organics and Cr(VI)

#### Experiment Section

**Chemicals and reagents.** 1,4-Dicyanobenzene (DCB), p-cyanophenol (*p*-CP), trifluoroethane sulfonic acid (TFMS) and 5, 5-dimethyl-1-pyrroline-N-oxide (DMPO) were obtained from Sigma-Aldrich Chemical Co., Ltd. Tetraethyl orthosilicate (TEOS), potassium dichromate ( $K_2Cr_2O_7$ ) and bisphenol A (BPA) were purchased from J&K Co. Ltd., (China). Tert-butyl alcohol (TBA), methanol (MeOH), ethanol (EtOH), disodium ethylenediaminetetraacetate (EDTA-2Na), and 2-tert-butyl-1,4-benzoquinone (BQ) were obtained from Sinopharm Chemical Reagent Co., Ltd. (Shanghai, China). Ammonium hydroxide ( $NH_3 \cdot H_2O$ , 25–28%  $NH_3$  basis) was supplied by Hangzhou Longshan Fine Chemical Co., Ltd. (Hangzhou, China). HPLC grade methanol were purchased from J&K Co. Ltd., (China). All the chemicals were of chemical grade or higher and were used without further purification. Ultrapure water was obtained from Milli-Q® ultrapure water purification systems (Milford, MA).

**Preparation of Pristine CTF.** Pristine CTF was synthesized by the mildly method. Typically, 2.5 mL of TFMS dripped into 4 mmol of DCB slowly and stirred swiftly for 1.5 h at 0 °C to gain a thick liquid, then the resultants were heated to 100 °C and kept for 20 min. Subsequently, the samples were collected by centrifugation and washed by 5 mL of ammonia solution, 5 mL of ethanol, 5 mL of deionized water in sequence for three times. At last, the obtained CTFs were drying at 60 °C under vacuum overnight.

**Preparation of STCH-CTFs.** STCH-CTFs were synthesized via simply mixt and grinded

the DCB and p-CP as precursors. In detail, 0.2 mmol of p-CP and 3.8 mmol of DCB (the mole fraction of p-CP ( $X_{p\text{-CP}}$ ) is 5%) were blended as precursors and dissolved in 2.5 mL of TFMS, which was then stirred at 0 °C for 1.5 h in a nitrogen atmosphere. Subsequently, the mixture was heated to 100 °C and maintained for 20 min. Finally, the products were collected by centrifugation and washed by 5 mL of ammonia solution, 5 mL of ethanol and 5 mL of deionized water in sequence for three times. At last, the obtained CTFs were drying at 60 °C under vacuum overnight and labeled as STCH-CTF<sub>5</sub>. Changing the mole fraction of p-CP in the precursor mixture to 10% (0.4 mmol of p-CP and 3.6 mmol of DCB), 15% (0.6 mmol of p-CP and 3.4 mmol of DCB), and 20% (0.8 mmol of p-CP and 3.2 mmol of DCB), the produced CTFs were labeled as STCH-CTF<sub>10</sub>, STCH-CTF<sub>15</sub>, and STCH-CTF<sub>20</sub>, respectively.

**Characterization.** The characteristics in the aspect of morphologies, surface composition and crystalline structure of the catalysts were investigated by scan and transmission electronic microscopy (SEM and TEM), X-ray diffraction (XRD), Brunauer–Emmett–Teller (BET) analyses and X-ray photoelectron spectroscopy (XPS). The morphology was characterized with scanning electron microscopy (SEM) (S-4800, Hitachi) and transmission electron microscopy (TEM, Tecnai G2 F30 S-Twin, Netherlands) equipped with an energy-dispersive X-ray spectroscopy (EDX) system (Genesis 4000, EDAX). The chemical compositions and electronic states of the prepared particles were determined by X-ray photoelectron spectroscopy (XPS) (PHI 5000 C, PerkinElmer) using Mg-K $\alpha$  radiation (1253.6 eV). The binding energies of the recorded XPS spectra were corrected according to the C 1s line at 284.6 eV. After subtracting the Shirley-type background, the core-level spectra were deconvoluted into their components

with mixed Gaussian–Lorentzian (20:80) shape lines using Casa XPS software. The crystallographic phases of the prepared catalysts were identified by X-ray diffraction (XRD) (SCINTAG X’TRA X-ray diffractometer, Thermo ARL) using Cu-K $\alpha$  radiation operating at 45 kV and 40 mA in the  $2\theta$  range of 10–80°. The functional groups were characterized by Fourier transform infrared (FTIR) spectroscopy (Nexus 670, USA). The specific surface areas of the materials were obtained via a N<sub>2</sub> adsorption–desorption and Brunauer–Emmett–Teller (BET) method with a Micrometric ASAP 2000. Solid-state <sup>13</sup>C CP MAS NMR measurements were carried out using a Bruker Avance II solid-state NMR spectrometer operating at a 300 MHz Larmor frequency equipped with a standard 4 mm magic angle spinning (MAS) double resonance probe head. Electron paramagnetic resonance (EPR) spectroscopy was performed on an EPR spectrometer (A300; Bruker, Germany) using 5,5-dimethyl-1-pyrrolidine N-oxide (DMPO) as a radical spin trapping reagent. The photoelectrochemical and electrochemical properties were determined by methods including UV-visible diffuse-reflectance spectroscopy (UV–vis DRS), periodic on/off photocurrent responses, electrochemical impedance spectroscopy (EIS) and linear sweep voltammetry (LSV), etc.

**Adsorption Experiments.** Typical adsorption experiments were conducted by dispersing STCH-CTFs (0.2 g L<sup>-1</sup>) in mixed solutions of BPA (0.005–0.2 mM) and Cr(VI) (0.01–0.6 mM) at 298 K. At regular time intervals, the suspension was sampled and filtered immediately by using 0.45  $\mu$ m membrane filters to remove the solid particles. The concentration of BPA was measured by high-performance liquid chromatography (HPLC; Waters Corporation, USA) equipped with a UV-vis detector. An Agilent Zorbax XDB-C18 column (150 mm  $\times$  4.6 mm, 5  $\mu$ m particle size) was used for separation with methanol-

water (70:30; v/v) at a flow rate of 1 mL min<sup>-1</sup> and an absorption wavelength of 225 nm.<sup>1</sup>

The concentration of Cr(VI) was detected using a Tu-1810 UV-visible spectrometer at  $\lambda_{\text{max}} = 540$  nm.<sup>2</sup> The adsorption kinetics of the catalysts were used by pseudo-second-order kinetic models. The Freundlich and Langmuir models were employed to fit the adsorption isotherms. The amount of BPA and Cr(VI) adsorbed were calculated by using the following equations:

$$\text{Langmuir isotherm: } q_e = \frac{q_m K_L C_0}{1 + K_L C_0}$$

$$\text{Freundlich isotherm: } q_e = K_F C_e^{1/n}$$

where  $q_e$  is the adsorbate amount at equilibrium (mol g<sup>-1</sup>),  $q_m$  is the maximum adsorption capacity corresponding to the monolayer full coverage (mol g<sup>-1</sup>),  $C_0$  is initial concentration in water (mol L<sup>-1</sup>),  $K_L$  is the Langmuir equilibrium constant (L mol<sup>-1</sup>),  $K_F$  is the Freundlich isotherm constant and  $n$  is an indicator of adsorption capacity (mol g<sup>-1</sup> (L mol<sup>-1</sup>)<sup>1/n</sup>)  $C_e$  is the final equilibrium concentration in water (mg L<sup>-1</sup>).

The pseudo-second order kinetic model was employed to characterize adsorption kinetics as follows:

$$\frac{t}{q_t} = \frac{1}{k_2 q_e^2} + \frac{t}{q_e}$$

where  $q_e$  is the adsorption capacity at equilibrium (mol g<sup>-1</sup>).

**Catalytic Degradation.** The degradation experiments were carried out in a 100 mL beaker at 298 K. STCH-CTFs (0.2 g L<sup>-1</sup>) were dispersed in a 100 mL Cr(VI)/BPA mixed solution and the concentration of Cr(VI) and BPA in the composite solution was 10 mg L<sup>-1</sup>. Experiments were measured under AM 1.5 (100 mW cm<sup>-2</sup>) conditions (300 W Xe lamp) to obtain a solar-like spectrum. To achieve adsorption–desorption equilibrium, the system

was stirred in the dark for 15 min. Aliquots were taken after definite intervals of time, and then were filtered out using 0.45  $\mu\text{m}$  PTFE syringe filter. The degradation tests of BPA and Cr(VI) were determined by HPLC and UV-visible spectrometry.<sup>3</sup> Tap water and natural water samples were employed as water matrices to further estimate the effect of target systems in practical application. The natural water sample was collected from Shang Tang Lake in Zhejiang (China) and filtrated with a 0.45  $\mu\text{m}$  membrane. Quenching tests were implemented by using EDTA-2Na, BQ and TBA. The designated quenchers should dissolve into the solution before adding of catalysts. The generation of  $\text{O}_2^{\cdot-}$  was determined by Electron paramagnetic resonance (EPR) spectroscopy (A300; Bruker, Germany) employing 5,5-dimethyl-1-pyrroline N-oxide (DMPO) as a radical spin-trapping reagent.

**DFT Calculations.** DFT calculations were carried out using the “Vienna ab initio simulation package” (VASP). The Perdew–Burke–Ernzerhof (PBE) functional was used within the spin-polarized generalized gradient approximation (GGA). The corresponding systems were optimised and further treated with restrictive optimisation to an energy minimum geometry. The k-points were sampled in a  $1 \times 2 \times 1$  Monkhorst-Pack grid in all calculations. The convergence criteria of self-consistent field tolerance, energy tolerance, maximum force tolerance and maximum displacement tolerance during the calculations were  $1.0 \times 10^{-6}$  Ha/atom,  $1.0 \times 10^{-5}$  Ha, 0.002 Ha/ $\text{\AA}$  and 0.005  $\text{\AA}$ , respectively.

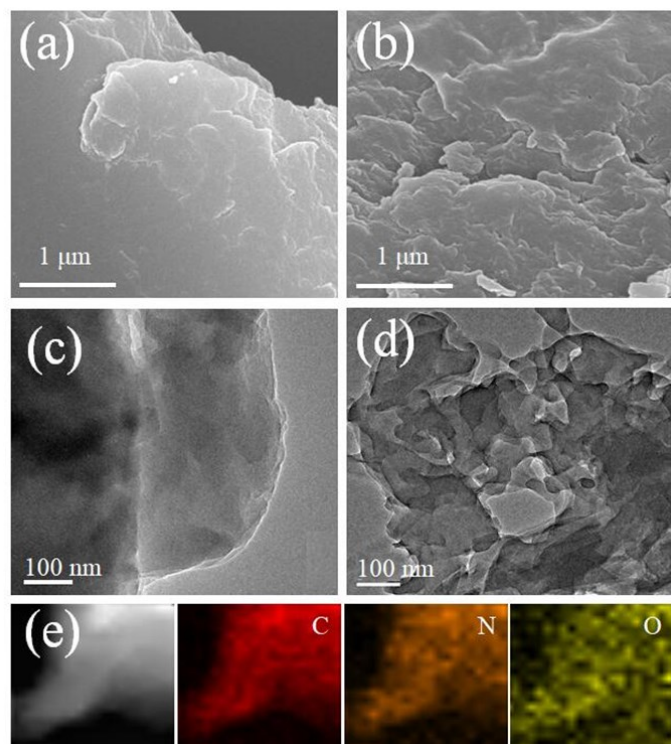


**Fig. S1.** SEM images of the pristine CTF (a) and STCH-CTF<sub>10</sub> (b); TEM images of the pristine CTF (c) and STCH-CTF<sub>10</sub> (d); and an elemental mapping of STCH-CTF<sub>10</sub> (e).

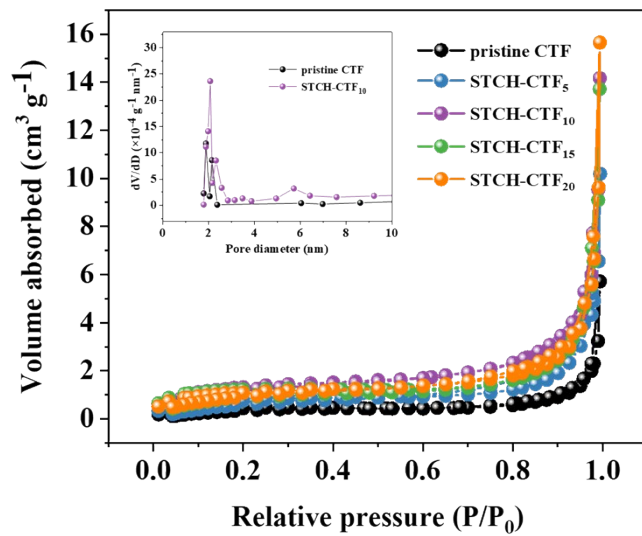


**Fig. S2.** N<sub>2</sub> adsorption–desorption isotherms (inset is pore size distribution) of pristine CTF and STCH-CTFs.

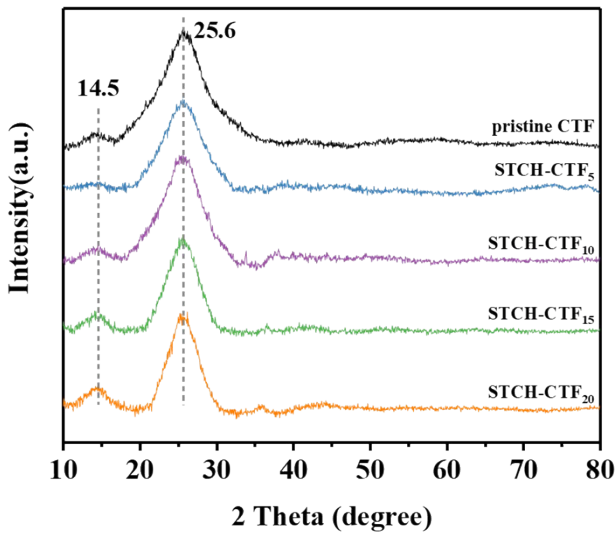


**Fig. S3.** XRD patterns of pristine CTF and STCH-CTFs.

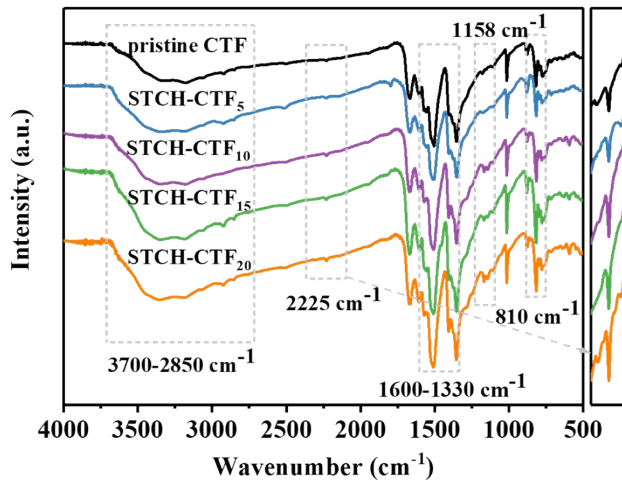


**Fig. S4.** FTIR spectra of pristine CTF and STCH-CTFs.

To provide further insight into the newly formed terminal groups, solid-state  $^{13}\text{C}$  MAS NMR measurements were carried out (Fig. S5). This ascertained the presence of  $\text{sp}^2$ -hybridized carbon species as part of benzene rings ( $\delta = 120\text{--}145 \text{ ppm}$ ) and  $\text{sp}^2$ -bonded carbon atoms in triazine heterocycles ( $\delta \approx 170 \text{ ppm}$ ). In addition, STCH-CTF samples showed carbon-oxygen bonds ( $\delta \approx 117 \text{ ppm}$ ), and the peak strength improved with the increase of *p*-CP content. These signals were consistent with the predicted  $^{13}\text{C}$ -NMR shifts, further indicating the presence of  $-\text{CN}$  and  $-\text{OH}$  groups in STCH-CTFs.

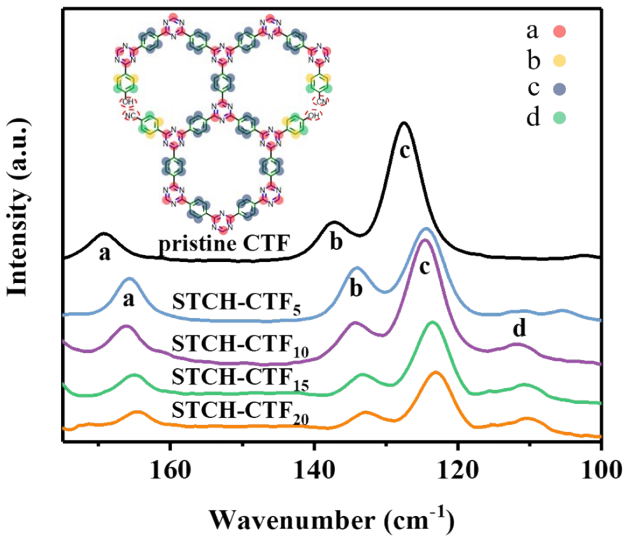


**Fig. S5.** Solid-state  $^{13}\text{C}$  NMR spectra of pristine CTF and STCH-CTFs.

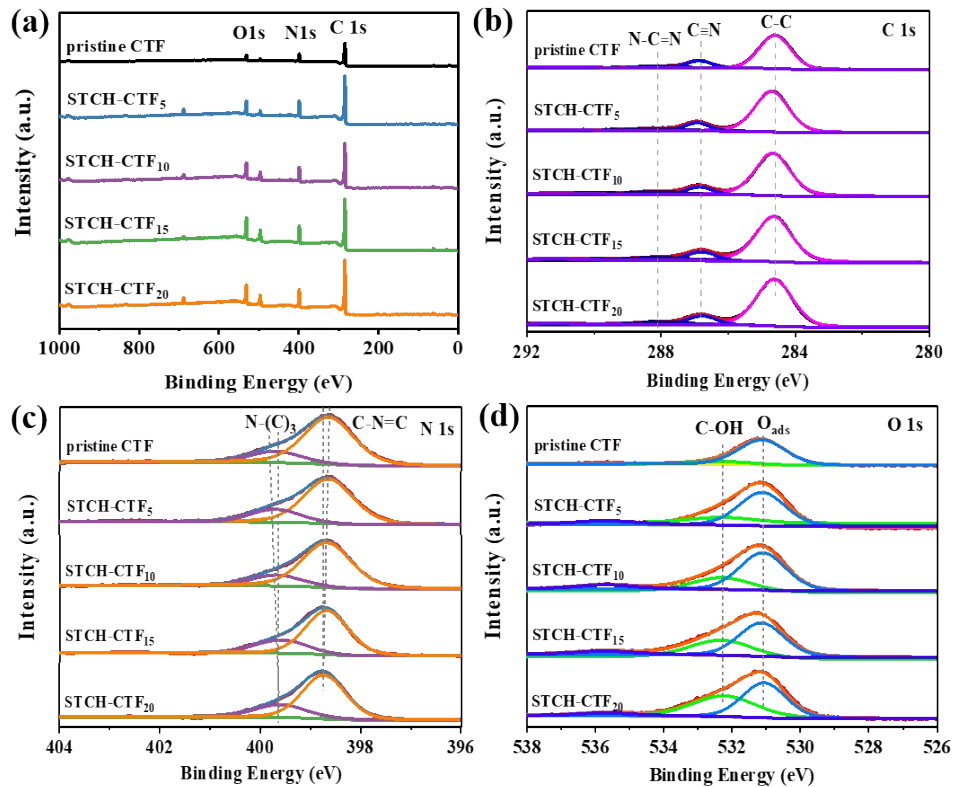


**Fig. S6.** XPS wide-scan spectrum (a), C 1s (b), N 1s (c) and O 1s (d) spectrum of pristine CTF and STCH-CTFs.

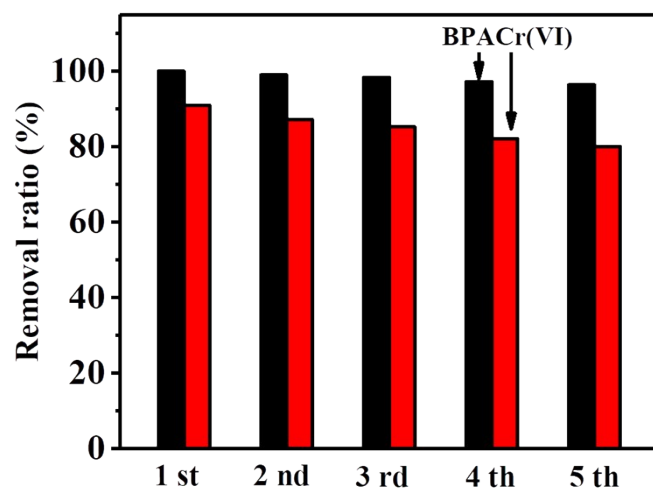


**Fig. S7.** Stability test of STCH-CTF<sub>10</sub> for BPA degradation and Cr(VI) reduction.

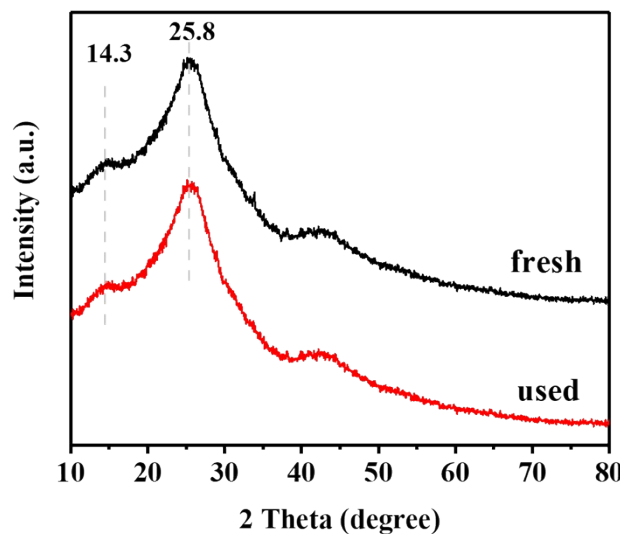


**Fig. S8.** XRD patterns of fresh and recycled STCH-CTF<sub>10</sub> or BPA degradation and Cr(VI) reduction.

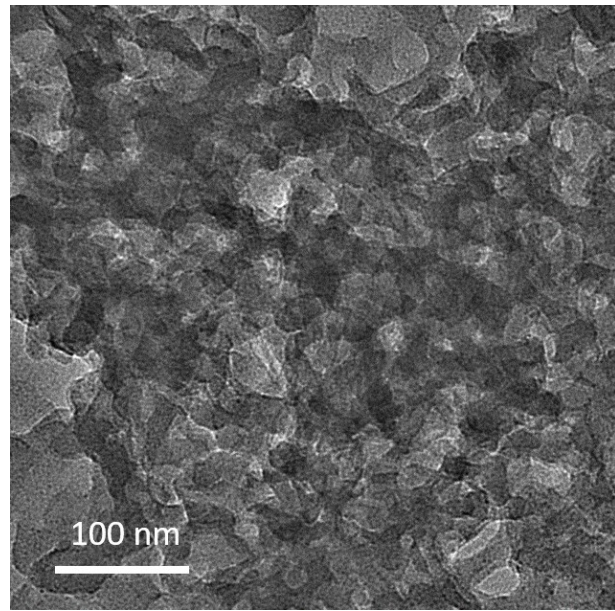


**Fig. S9.** TEM images for STCH-CTF<sub>10</sub> obtained after the fifth run for BPA degradation and Cr(VI) reduction.

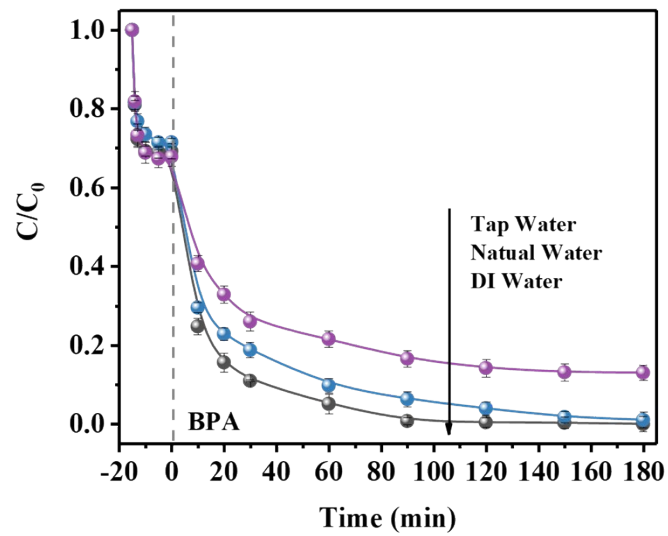


**Fig. S10.** BPA degradation by the STCH-CTF<sub>10</sub> system in different water matrices.

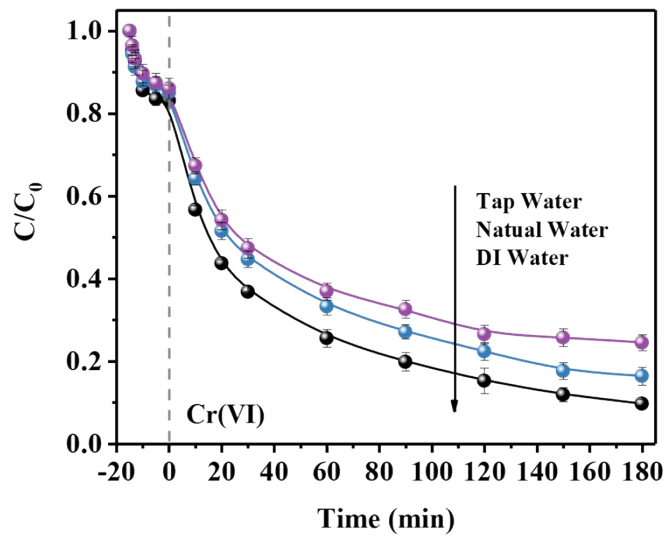


**Fig. S11.** Cr(VI) reduction by the STCH-CTF<sub>10</sub> system in different water matrices.

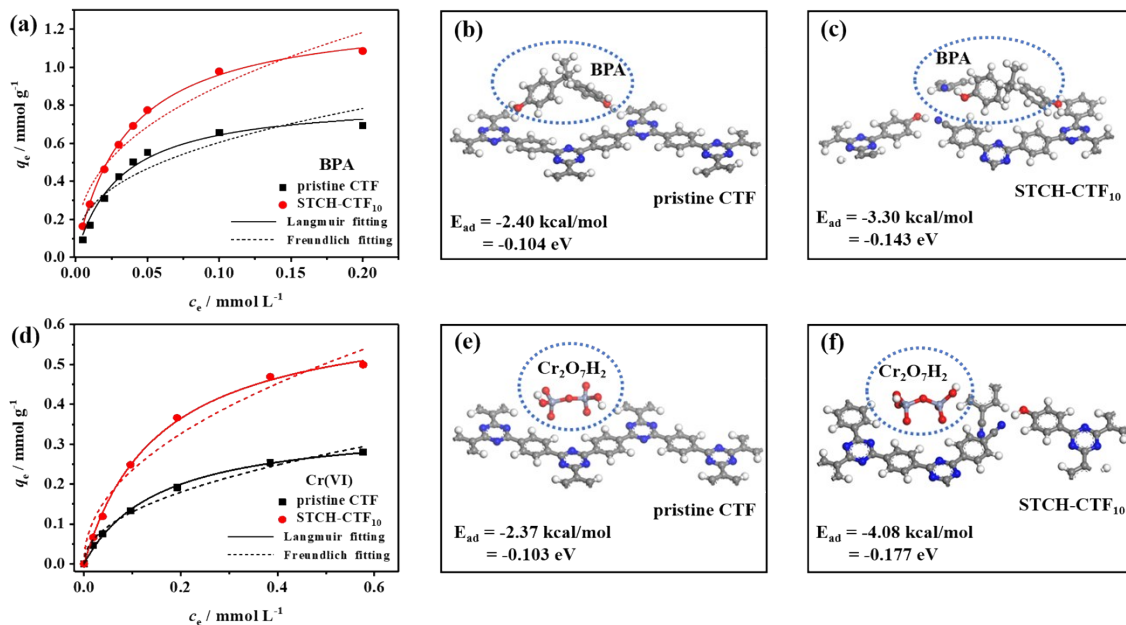


**Fig. S12.** Adsorption isotherms of BPA (a) and Cr(VI) (d) on the pristine CTF and STCH-CTF<sub>10</sub> at 298 K, theoretical calculation of BPA (b, c) and Cr(VI) (e, f) adsorption on the surface of the pristine CTF and STCH-CTF<sub>10</sub>.

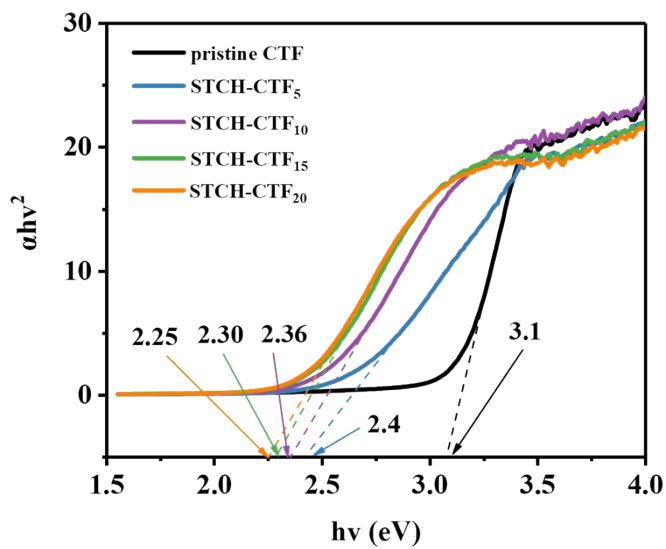


**Fig. S13.** Kubelka-Munk plots converted from the UV–vis DRS spectra of the pristine CTF and STCH-CTFs.

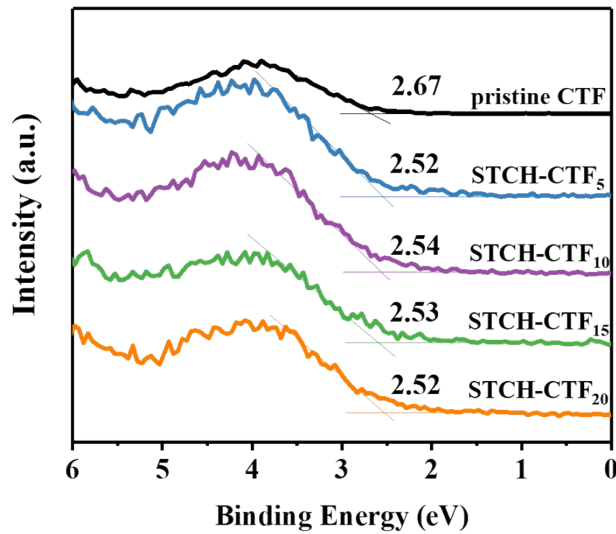


**Fig. S14.** VB-XPS spectra for pristine CTF and STCH-CTFs.

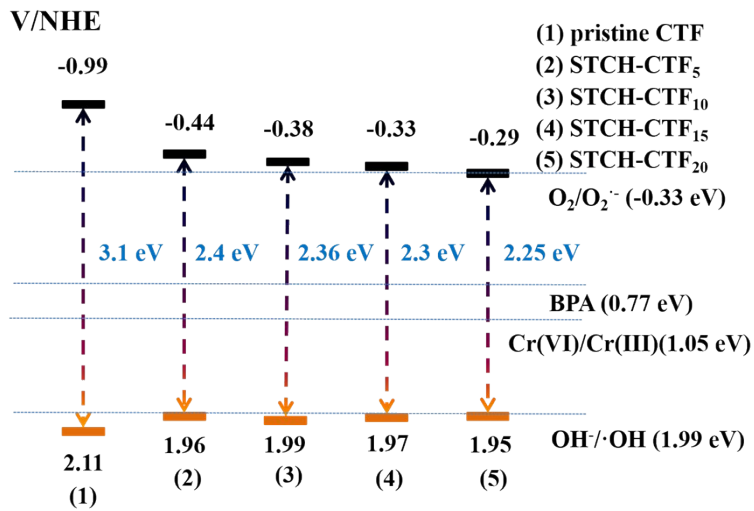


**Fig. S15.** Band structure alignments of the pristine CTF and STCH-CTFs.

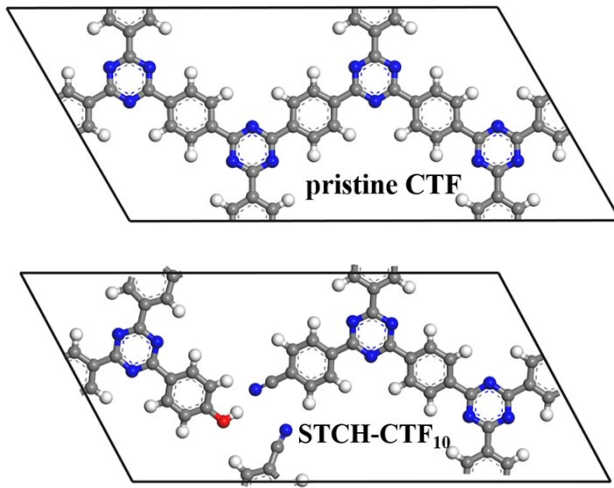


**Fig. S16.** Top view of optimized geometries of pristine CTF and STCH-CTF<sub>10</sub>.

Room-temperature EPR spectra (Fig. S17) were also recorded to compare the electronic band structures of the pristine CTF and STCH-CTFs cases.<sup>4</sup> The higher EPR signal intensity of STCH-CTF<sub>10</sub> than pristine CTF and other STCH-CTFs demonstrated the accelerated generation of unpaired electrons along with the introduction of appropriate amount -CN and -OH groups at the edge sites.<sup>5</sup> This was probably due to the redistribution of electrons caused by the addition of structural terminations, which facilitates the photoinduced formation of charge carriers and benefits the generation of unpaired electrons for photocatalytic reactions.

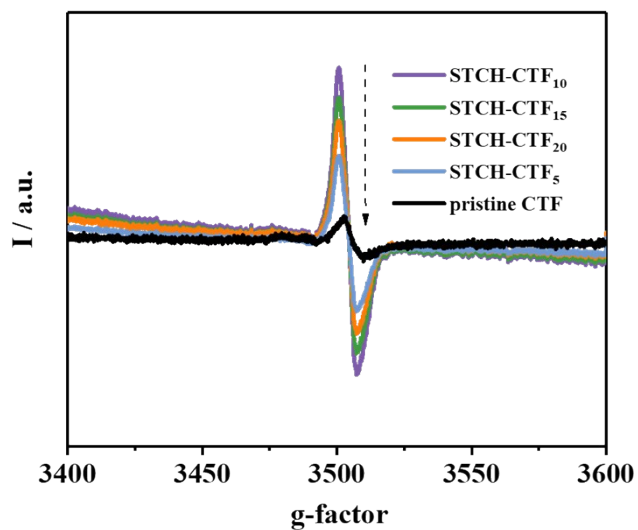


**Fig. S17.** Room-temperature EPR spectra of pristine CTF and STCH-CTFs.

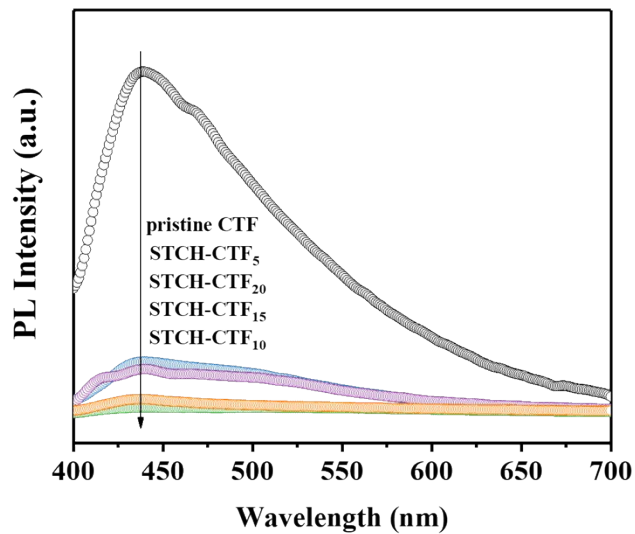


**Fig. S18.** Photoluminescence emission peak of pristine CTF and STCH-CTFs.

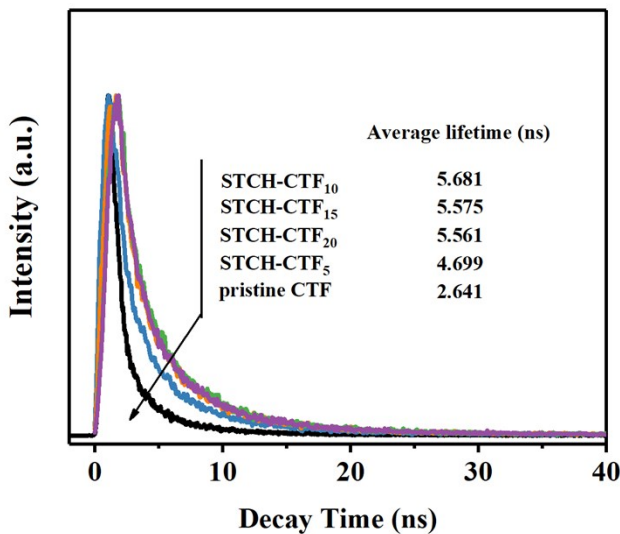


**Fig. S19.** Time-resolved fluorescence decay of pristine CTF and STCH-CTFs.

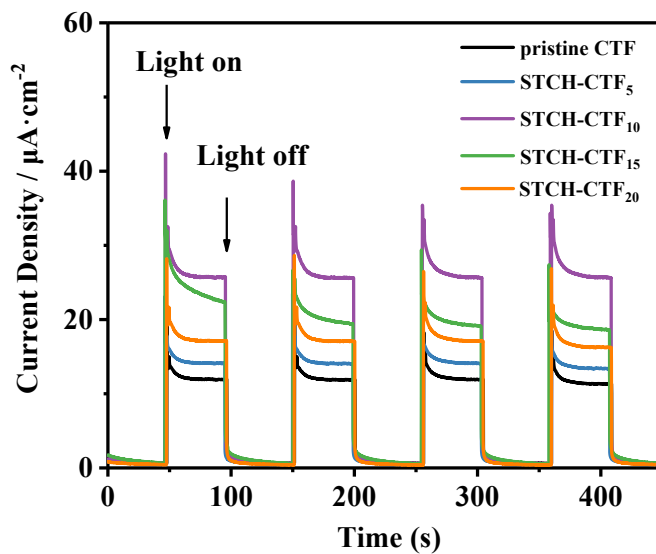


**Fig. S20.** Photocurrent of pristine CTF and STCH-CTFs.

Samples examined by measuring the photocurrent using LSV under visible light and in the dark irradiation (Fig. S21) showed a similar trend to those of photocurrent, demonstrating that more efficient charges transfer processes of STCH-CTFs were achieved. The results illustrated that the appropriate content of structural terminations with -CN and -OH groups in STCH-CTF<sub>10</sub> could dramatically accelerate the transfer behaviors

of charge carriers in addition to enhancing the visible-light utilization capability by altering the electronic states and optical properties, making it an excellent polymeric semiconductor to drive the simultaneous photocatalysis of Cr(VI) reduction and BPA oxidation.

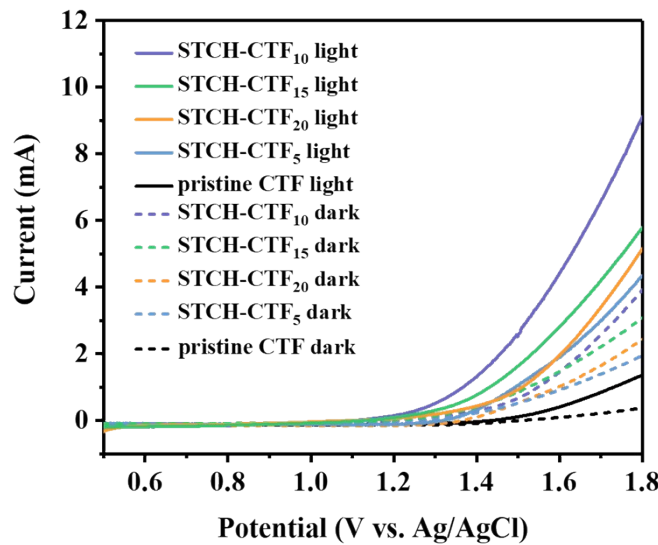


**Fig. S21.** LSV curves of pristine CTF and STCH-CTFs in light (solid line) or in dark (dotted line).

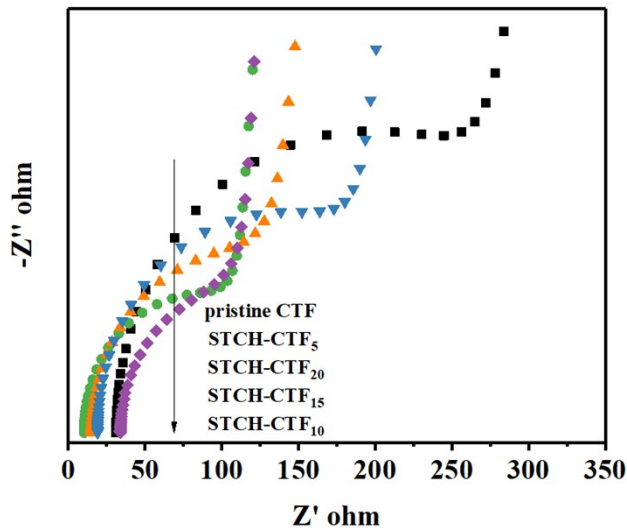


**Fig. S22.** Nyquist plots in the dark of the pristine CTF and STCH-CTFs.

To confirm the presence of  $O_2^{+}$  in photocatalytic system, EPR spectroscopy was

performed using DMPO as a radical spin trapping reagent, which was conducted by using MeOH as the solvent instead of water. As shown in Fig. S23, the characteristic signals of DMPO/ $O_2^{-}$  adduct with hyperfine splitting constants  $\alpha_N = 14.3$  G,  $\alpha_H = 11.2$  G and  $\alpha_H = 1.3$  G were obtained, suggesting that  $O_2^{-}$  was produced in photocatalytic systems.<sup>6,7</sup> The DMPO/ $O_2^{-}$  six distinct characteristic peaks (labeled as blue dots) implied that  $O_2^{-}$  also participated in Cr(VI) reduction ( $Cr(VI) + O_2^{-} \rightarrow Cr(III) + O_2$ ) and BPA oxidation ( $O_2 + e^- \rightarrow O_2^{-}; O_2^{-} + 2H^+ + e^- \rightarrow H_2O_2; H_2O_2 + e^- \rightarrow \cdot OH + HO^-; BPA + \cdot OH \rightarrow \text{products}$ ), which was consistent with the results of quenching experiment. Thus, DMPO EPR technique could also indicate that  $O_2^{-}$  contributes to both BPA oxidation and Cr(VI) reduction.

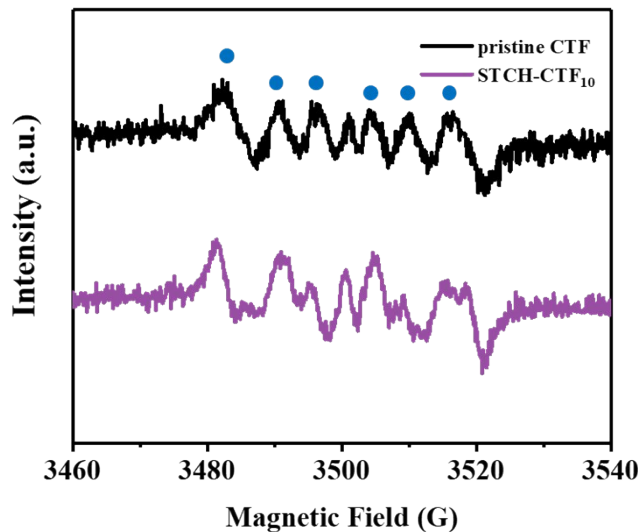


**Fig. S23.** EPR spectra of DMPO spin-trapping for  $O_2^{-}$  under visible light irradiation of the pristine CTF and STCH- $CTF_{10}$ .

**Table S1** Summarized XPS data for pristine CTF and STCH- $CTF_S$ , surface C/N/O atom ratios determined from quantitative analyses were provided.

Sample	C [Atomic %]	N [Atomic %]	O [Atomic %]
Pristine CTF	75.3	15.0	7.4
STCH-CTF <sub>5</sub>	70.4	12.7	13.1
STCH-CTF <sub>10</sub>	69.1	13.0	13.7
STCH-CTF <sub>15</sub>	70.0	13.1	13.1
STCH-CTF <sub>20</sub>	73.9	14.2	10.0

**Table S2** Comparison of the Cr(VI) reduction efficiency between different polymer-based organic photocatalysts.

Organic photocatalysts (Dosage)	Light source	Cr(VI) (C <sub>0</sub> , mg L <sup>-1</sup> )	t (h)	η (%)	Reduction efficiency (mg L <sup>-1</sup> g <sup>-1</sup> h <sup>-1</sup> )	Ref.
g-C <sub>3</sub> N <sub>4</sub> (1 g L <sup>-1</sup> )	300 W Xe lamp with a cutoff filter (>420 nm)	10	3	97	3.23	8
N <sub>2</sub> -g-C <sub>3</sub> N <sub>4</sub> (0.5 g L <sup>-1</sup> )	300 W Xe lamp with a cutoff filter (>420 nm)	10	2	70	7	9
g-C <sub>3</sub> N <sub>4</sub> -Br <sub>20</sub> (1 g L <sup>-1</sup> )	300 W Xe lamp with a cutoff filter (>420 nm)	7	2	60	2.1	10
(P, Mo)-g-C <sub>3</sub> N <sub>4</sub> (1.25 g L <sup>-1</sup> )	300 W Xe lamp with a cutoff filter (>420 nm)	14	2	95	5.36	11
PCN-S (1 g L <sup>-1</sup> )	300 W Xe lamp with a cutoff filter (>400 nm)	20	2	90	9	12
α-Fe <sub>2</sub> O <sub>3</sub> /g-C <sub>3</sub> N <sub>4</sub> -0.5 (2 g L <sup>-1</sup> )	300 W Xe lamp with a cutoff filter (>400 nm)	10	2.5	98	1.96	13
STCH-CTF <sub>10</sub> (0.2 g L <sup>-1</sup> )	300 W Xe lamp with a cutoff filter (>400 nm)	10	3	75	12.5	this work
STCH-CTF <sub>10</sub> (0.2 g L <sup>-1</sup> )	300 W Xe lamp with a cutoff filter (AM 1.5, 100 mW cm <sup>-2</sup> )	10	3	90	15	this work

$$\text{Reduction efficiency: } Q_e = \frac{C_0 \eta}{C_{\text{cat.}} t};$$

$C_0$ : initial concentration of Cr(VI);

$C_{\text{Cat.}}$ : concentration of photocatalyst;

t: reaction time;

$\eta$ : degree of reduction.

**Table S3** Reaction rate constant, BET surface area and specific activity for Cr(VI) reduction by pristine CTF and STCH-CTFs.

sample	pristine CTF	STCH- CTF <sub>5</sub>	STCH-CTF <sub>10</sub>	STCH-CTF <sub>15</sub>	STCH-CTF <sub>20</sub>
k (min <sup>-1</sup> )	0.0092	0.0112	0.0356	0.0286	0.0205
BET (m <sup>2</sup> g <sup>-1</sup> )	2.59	2.72	4.53	3.87	3.67
Pore Volume (cm <sup>3</sup> g <sup>-1</sup> )	0.003	0.020	0.022	0.020	0.024
specific activity (g <sup>1</sup> cm <sup>-2</sup> min <sup>-1</sup> )	3.56*10 <sup>-3</sup>	4.12*10 <sup>-3</sup>	7.86*10 <sup>-3</sup>	7.39*10 <sup>-3</sup>	5.59*10 <sup>-3</sup>

As shown in Table S3, the specific activity of STCH-CTF<sub>10</sub> still far exceeds those of pristine CTF and other STCH-CTF samples, manifesting that the catalytic activity was not mainly affected by surface area. This demonstrated that the structural terminations in the framework are the critical factor for the enhanced photocatalytic performance.

**Table S4** Calculated kinetic parameters of the pseudo-second-order model for BPA on the pristine CTF and STCH-CTF<sub>10</sub>.

Adsorbents	Pseudo-second-order parameters <sup>a</sup>
------------	---

	$k_2$	$q_e$ (mol/g)	$R^2$
Pristine CTF	15.566	0.767	0.997
STCH-CTF <sub>10</sub>	16.928	0.549	0.998

<sup>a</sup> Pseudo-second-order model:  $t/qt = 1/k_2q_e^2 + t/q_e$

**Table S5** Calculated kinetic parameters of the pseudo-second-order model for Cr(VI) on the pristine CTF and STCH-CTF<sub>10</sub>.

Adsorbents	Pseudo-second-order parameters <sup>a</sup>		
	$k_2$	$q_e$ (mol/g)	$R^2$
Pristine CTF	10.183	0.369	0.999
STCH-CTF <sub>10</sub>	12.852	0.174	0.999

<sup>a</sup> Pseudo-second-order model:  $t/qt = 1/k_2q_e^2 + t/q_e$

**Table S6** Calculated constants of the Langmuir and Freundlich models for BPA adsorption on pristine CTF and STCH-CTF<sub>10</sub>.

Adsorbents	Langmuir parameters <sup>a</sup>		Freundlich parameters <sup>b</sup>	
	$q_m$ (mol/g)	$R^2$	$K_F$ (mg <sup>1-1/n</sup> L <sup>1/n</sup> /g)	$R^2$
Pristine CTF	0.838	0.991	1.428	0.847
STCH-CTF <sub>10</sub>	1.294	0.998	2.226	0.932

$$q_e = \frac{q_m K_L C_0}{1 + K_L C_0} \quad \text{Eq. (1)}$$

<sup>a</sup> Langmuir model:

$$q_e = K_F C_e^{1/n} \quad \text{Eq. (2)}$$

**Table S7** Calculated constants of the Langmuir and Freundlich models for Cr(VI) adsorption on pristine CTF and STCH-CTF<sub>10</sub>.

Adsorbents	Langmuir parameters <sup>a</sup>		Freundlich parameters <sup>b</sup>	
	$q_m$	$R^2$	$K_F$	$R^2$

	(mol/g)	(mg <sup>1-1/n</sup> L <sup>1/n</sup> /g)		
Pristine CTF	0.353	0.991	0.379	0.985
STCH-CTF <sub>10</sub>	0.645	0.998	0.697	0.969

$$q_e = \frac{q_m K_L C_0}{1 + K_L C_0} \quad \text{Eq. (1)}$$

<sup>a</sup> Langmuir model:

$$q_e = K_F C_e^{1/n} \quad \text{Eq. (2)}$$

## DFT calculations

### Molecular Coordinates

#### pristine CTF (periodic structure)

		_cell_length_a			29.5300			
		_cell_length_b			14.7650			
		_cell_length_c			4.0000			
		_cell_angle_alpha			90.0000			
		_cell_angle_beta			90.0000			
		_cell_angle_gamma			120.0000			
N13	N	0.13982	1.55929	0.40429	0.01267	Uiso	1.00	
N14	N	0.22035	1.72036	0.40429	0.01267	Uiso	1.00	
N15	N	0.13980	1.72039	0.40429	0.01267	Uiso	1.00	
N16	N	0.36018	1.44071	0.40429	0.01267	Uiso	1.00	
N17	N	0.27964	1.27964	0.40429	0.01267	Uiso	1.00	
N18	N	0.36020	1.27961	0.40429	0.01267	Uiso	1.00	
N19	N	0.63982	1.55929	0.40429	0.01267	Uiso	1.00	
N20	N	0.72035	1.72036	0.40429	0.01267	Uiso	1.00	
N21	N	0.63980	1.72039	0.40429	0.01267	Uiso	1.00	
N22	N	0.86018	1.44071	0.40429	0.01267	Uiso	1.00	
N23	N	0.77965	1.27964	0.40429	0.01267	Uiso	1.00	
N24	N	0.86020	1.27961	0.40429	0.01267	Uiso	1.00	
C49	C	0.19263	1.61475	0.40429	0.01267	Uiso	1.00	

C50	C	0.22197	1.55606	0.40429	0.01267	Uiso	1.00
C51	C	0.19261	1.77049	0.40429	0.01267	Uiso	1.00
C52	C	0.22197	1.88788	0.40429	0.01267	Uiso	1.00
C53	C	0.11475	1.61478	0.40429	0.01267	Uiso	1.00
C54	C	0.05606	1.55606	0.40429	0.01267	Uiso	1.00
C55	C	0.30737	1.38525	0.40429	0.01267	Uiso	1.00
C56	C	0.27803	1.44394	0.40429	0.01267	Uiso	1.00
C57	C	0.30739	1.22951	0.40429	0.01267	Uiso	1.00
C58	C	0.27803	1.11212	0.40429	0.01267	Uiso	1.00
C59	C	0.38525	1.38522	0.40429	0.01267	Uiso	1.00
C60	C	0.44394	1.44394	0.40429	0.01267	Uiso	1.00
C61	C	0.19568	1.44594	0.40429	0.01267	Uiso	1.00
C62	C	0.27703	1.94541	0.40429	0.01267	Uiso	1.00
C63	C	0.02729	1.60864	0.40429	0.01267	Uiso	1.00
C64	C	0.30432	1.55406	0.40429	0.01267	Uiso	1.00
C65	C	0.22297	1.05459	0.40429	0.01267	Uiso	1.00
C66	C	0.47271	1.39136	0.40429	0.01267	Uiso	1.00
C67	C	0.22297	1.39136	0.40429	0.01267	Uiso	1.00
C68	C	0.47271	1.55406	0.40429	0.01267	Uiso	1.00
C69	C	0.30432	1.05458	0.40429	0.01267	Uiso	1.00
C70	C	0.27703	1.60864	0.40429	0.01267	Uiso	1.00
C71	C	0.02729	1.44594	0.40429	0.01267	Uiso	1.00
C72	C	0.19568	1.94542	0.40429	0.01267	Uiso	1.00
C73	C	0.69263	1.61475	0.40429	0.01267	Uiso	1.00
C74	C	0.72197	1.55606	0.40429	0.01267	Uiso	1.00
C75	C	0.69261	1.77049	0.40429	0.01267	Uiso	1.00
C76	C	0.72197	1.88788	0.40429	0.01267	Uiso	1.00
C77	C	0.61475	1.61478	0.40429	0.01267	Uiso	1.00
C78	C	0.55606	1.55606	0.40429	0.01267	Uiso	1.00
C79	C	0.80737	1.38525	0.40429	0.01267	Uiso	1.00
C80	C	0.77803	1.44394	0.40429	0.01267	Uiso	1.00

C81	C	0.80739	1.22951	0.40429	0.01267	Uiso	1.00
C82	C	0.77803	1.11212	0.40429	0.01267	Uiso	1.00
C83	C	0.88525	1.38522	0.40429	0.01267	Uiso	1.00
C84	C	0.94394	1.44394	0.40429	0.01267	Uiso	1.00
C85	C	0.69568	1.44594	0.40429	0.01267	Uiso	1.00
C86	C	0.77703	1.94541	0.40429	0.01267	Uiso	1.00
C87	C	0.52729	1.60864	0.40429	0.01267	Uiso	1.00
C88	C	0.80432	1.55406	0.40429	0.01267	Uiso	1.00
C89	C	0.72297	1.05459	0.40429	0.01267	Uiso	1.00
C90	C	0.97271	1.39136	0.40429	0.01267	Uiso	1.00
C91	C	0.72297	1.39136	0.40429	0.01267	Uiso	1.00
C92	C	0.97271	1.55406	0.40429	0.01267	Uiso	1.00
C93	C	0.80432	1.05458	0.40429	0.01267	Uiso	1.00
C94	C	0.77703	1.60864	0.40429	0.01267	Uiso	1.00
C95	C	0.52729	1.44594	0.40429	0.01267	Uiso	1.00
C96	C	0.69568	1.94542	0.40429	0.01267	Uiso	1.00
H25	H	0.15307	1.40276	0.40429	0.01267	Uiso	1.00
H26	H	0.29863	1.90338	0.40429	0.01267	Uiso	1.00
H27	H	0.04830	1.69387	0.40429	0.01267	Uiso	1.00
H28	H	0.34693	1.59724	0.40429	0.01267	Uiso	1.00
H29	H	0.20137	1.09662	0.40429	0.01267	Uiso	1.00
H30	H	0.45170	1.30613	0.40429	0.01267	Uiso	1.00
H31	H	0.20138	1.30614	0.40429	0.01267	Uiso	1.00
H32	H	0.45169	1.59725	0.40429	0.01267	Uiso	1.00
H33	H	0.34693	1.09661	0.40429	0.01267	Uiso	1.00
H34	H	0.29862	1.69386	0.40429	0.01267	Uiso	1.00
H35	H	0.04831	1.40275	0.40429	0.01267	Uiso	1.00
H36	H	0.15307	1.90339	0.40429	0.01267	Uiso	1.00
H37	H	0.65307	1.40276	0.40429	0.01267	Uiso	1.00
H38	H	0.79863	1.90338	0.40429	0.01267	Uiso	1.00
H39	H	0.54830	1.69387	0.40429	0.01267	Uiso	1.00

H40	H	0.84693	1.59724	0.40429	0.01267	Uiso	1.00
H41	H	0.70137	1.09662	0.40429	0.01267	Uiso	1.00
H42	H	0.95170	1.30613	0.40429	0.01267	Uiso	1.00
H43	H	0.70138	1.30614	0.40429	0.01267	Uiso	1.00
H44	H	0.95169	1.59725	0.40429	0.01267	Uiso	1.00
H45	H	0.84693	1.09661	0.40429	0.01267	Uiso	1.00
H46	H	0.79862	1.69386	0.40429	0.01267	Uiso	1.00
H47	H	0.54831	1.40275	0.40429	0.01267	Uiso	1.00
H48	H	0.65307	1.90339	0.40429	0.01267	Uiso	1.00

### STCH-CTF<sub>10</sub> (periodic structure)

		_cell_length_a			29.5300		
		_cell_length_b			14.7650		
		_cell_length_c			4.0000		
		_cell_angle_alpha			90.0000		
		_cell_angle_beta			90.0000		
		_cell_angle_gamma			120.0000		
N13	N	0.12123	1.55065	0.40546	0.01267	Uiso	1.00
N14	N	0.20398	1.70279	0.49234	0.01267	Uiso	1.00
N15	N	0.12622	1.71515	0.48607	0.01267	Uiso	1.00
N16	N	0.36687	1.46958	0.33913	0.01267	Uiso	1.00
N17	N	0.36693	1.26535	0.12516	0.01267	Uiso	1.00
N18	N	0.64949	1.59332	0.44985	0.01267	Uiso	1.00
N19	N	0.73234	1.74415	0.56825	0.01267	Uiso	1.00
N20	N	0.65715	1.76102	0.48635	0.01267	Uiso	1.00
N21	N	0.84819	1.43240	0.47542	0.01267	Uiso	1.00
N22	N	0.76718	1.27194	0.50398	0.01267	Uiso	1.00
N23	N	0.84783	1.27134	0.46465	0.01267	Uiso	1.00
C49	C	0.17355	1.59897	0.43879	0.01267	Uiso	1.00
C50	C	0.19737	1.53292	0.41520	0.01267	Uiso	1.00
C51	C	0.17881	1.75746	0.50301	0.01267	Uiso	1.00

C52	C	0.21201	1.87343	0.53042	0.01267	Uiso	1.00
C53	C	0.09930	1.61038	0.44145	0.01267	Uiso	1.00
C54	C	0.04110	1.55282	0.43477	0.01267	Uiso	1.00
C55	C	0.24104	1.40222	0.37295	0.01267	Uiso	1.00
C56	C	0.33386	1.17904	0.17160	0.01267	Uiso	1.00
C57	C	0.29737	1.07124	0.22791	0.01267	Uiso	1.00
C58	C	0.41150	1.49932	0.31761	0.01267	Uiso	1.00
C59	C	0.46610	1.53667	0.31219	0.01267	Uiso	1.00
C60	C	0.16867	1.43161	0.27838	0.01267	Uiso	1.00
C61	C	0.26693	1.92147	0.54297	0.01267	Uiso	1.00
C62	C	0.01199	1.60412	0.45212	0.01267	Uiso	1.00
C63	C	0.26974	1.50257	0.51670	0.01267	Uiso	1.00
C64	C	0.24540	1.03513	0.32738	0.01267	Uiso	1.00
C65	C	0.48461	1.46689	0.37086	0.01267	Uiso	1.00
C66	C	0.19022	1.36739	0.25394	0.01267	Uiso	1.00
C67	C	0.50113	1.64409	0.26712	0.01267	Uiso	1.00
C68	C	0.31569	1.00038	0.18564	0.01267	Uiso	1.00
C69	C	0.24821	1.56718	0.53279	0.01267	Uiso	1.00
C70	C	0.01413	1.44277	0.41633	0.01267	Uiso	1.00
C71	C	0.18951	1.93772	0.53625	0.01267	Uiso	1.00
C72	C	0.70129	1.64037	0.51244	0.01267	Uiso	1.00
C73	C	0.72485	1.57202	0.51804	0.01267	Uiso	1.00
C74	C	0.70819	1.80113	0.55580	0.01267	Uiso	1.00
C75	C	0.73738	1.91569	0.61739	0.01267	Uiso	1.00
C76	C	0.62966	1.65752	0.43722	0.01267	Uiso	1.00
C77	C	0.57312	1.61333	0.37272	0.01267	Uiso	1.00
C78	C	0.79580	1.37747	0.49613	0.01267	Uiso	1.00
C79	C	0.76981	1.44174	0.51063	0.01267	Uiso	1.00
C80	C	0.79525	1.22230	0.48947	0.01267	Uiso	1.00
C81	C	0.76710	1.10544	0.50561	0.01267	Uiso	1.00
C82	C	0.87275	1.37669	0.45984	0.01267	Uiso	1.00

C83	C	0.93066	1.43677	0.44190	0.01267	Uiso	1.00
C84	C	0.69353	1.46298	0.47543	0.01267	Uiso	1.00
C85	C	0.79222	1.97430	0.62536	0.01267	Uiso	1.00
C86	C	0.55432	1.68167	0.29876	0.01267	Uiso	1.00
C87	C	0.80092	1.55063	0.55636	0.01267	Uiso	1.00
C88	C	0.71223	1.04501	0.52744	0.01267	Uiso	1.00
C89	C	0.95984	1.38559	0.42024	0.01267	Uiso	1.00
C90	C	0.71555	1.39866	0.47400	0.01267	Uiso	1.00
C91	C	0.95758	1.54688	0.45431	0.01267	Uiso	1.00
C92	C	0.79559	1.05226	0.50305	0.01267	Uiso	1.00
C93	C	0.77893	1.61465	0.56194	0.01267	Uiso	1.00
C94	C	0.53806	1.50561	0.39928	0.01267	Uiso	1.00
C95	C	0.70896	1.96834	0.65831	0.01267	Uiso	1.00
H25	H	0.29928	1.37850	0.36463	0.01267	Uiso	1.00
H26	H	0.12932	1.40528	0.18591	0.01267	Uiso	1.00
H27	H	0.28452	1.87182	0.53906	0.01267	Uiso	1.00
H28	H	0.03264	1.68932	0.46550	0.01267	Uiso	1.00
H29	H	0.30881	1.52892	0.61429	0.01267	Uiso	1.00
H30	H	0.23152	1.09066	0.35804	0.01267	Uiso	1.00
H31	H	0.45651	1.38368	0.39443	0.01267	Uiso	1.00
H32	H	0.16879	1.29019	0.13873	0.01267	Uiso	1.00
H33	H	0.48627	1.69693	0.21384	0.01267	Uiso	1.00
H34	H	0.35590	1.02932	0.10505	0.01267	Uiso	1.00
H35	H	0.27030	1.64505	0.64233	0.01267	Uiso	1.00
H36	H	0.03689	1.40330	0.40263	0.01267	Uiso	1.00
H37	H	0.14703	1.90127	0.52755	0.01267	Uiso	1.00
H38	H	0.65154	1.42957	0.44136	0.01267	Uiso	1.00
H39	H	0.81462	1.93430	0.59702	0.01267	Uiso	1.00
H40	H	0.58223	1.76484	0.27295	0.01267	Uiso	1.00
H41	H	0.84296	1.58408	0.58586	0.01267	Uiso	1.00
H42	H	0.68946	1.08470	0.53067	0.01267	Uiso	1.00

H43	H	0.93932	1.30040	0.40909	0.01267	Uiso	1.00
H44	H	0.69096	1.31436	0.44058	0.01267	Uiso	1.00
H45	H	0.93500	1.58676	0.46826	0.01267	Uiso	1.00
H46	H	0.83809	1.09803	0.48602	0.01267	Uiso	1.00
H47	H	0.80341	1.69879	0.59812	0.01267	Uiso	1.00
H48	H	0.55325	1.45324	0.45094	0.01267	Uiso	1.00
H49	H	0.66641	1.92269	0.65725	0.01267	Uiso	1.00
O1	O	0.26047	1.33658	0.34484	0.01267	Uiso	1.00

pristine CTF (molecular fragment)

Charge = 0

Multiplicity = 1

N		4.48577610	7.99314953	-0.00010903
N		2.61855485	6.53008461	-0.00022197
N		2.27853430	8.87787060	-0.00023944
N		6.96563956	0.99753004	0.00009195
N		8.82881275	2.46575470	0.00011300
N		9.16626622	0.11171064	0.00001768
C		3.93972239	6.76094766	-0.00012111
C		4.85192539	5.59641962	-0.00005030
C		1.82257856	7.60956201	-0.00033105
C		0.35852167	7.39756408	-0.00021161
C		3.60640013	8.99492757	-0.00018105
C		7.50244252	2.22662702	0.00022020
C		6.58683427	3.38846525	0.00011252
C		9.59401586	1.37423298	-0.00008331
C		7.82605213	-0.03125569	0.00004082
C		7.27328141	-1.40347883	0.00001580
C		6.24308443	5.78783197	0.00002772
H		6.63390019	6.79814861	0.00003365

C	-0.17155120	6.09690758	-0.00020257
H	0.50761523	5.25324102	-0.00029485
C	5.19540669	3.19724517	0.00002560
H	4.80409337	2.18728651	0.00003457
C	8.13452225	-2.51263831	0.00000824
H	9.20485049	-2.34556331	0.00002012
C	7.10186074	4.69492645	0.00010448
H	8.17599583	4.83554051	0.00017268
C	5.88411022	-1.61060208	0.00000055
H	5.22487695	-0.75120003	0.00000583
C	4.33703454	4.28963462	-0.00005059
H	3.26314677	4.14837711	-0.00010450
C	-0.51519659	8.49696929	-0.00009500
H	-0.09944956	9.49728178	-0.00010688
N	6.54947975	-6.41262430	-0.00000067
N	4.67924463	-7.88124849	-0.00003523
N	4.34651074	-5.53245236	-0.00008989
C	5.98658841	-7.62095250	0.00004081
C	3.88556124	-6.79195157	-0.00012805
C	2.42083441	-6.99936387	-0.00007197
C	5.67945716	-5.38331116	-0.00004434
C	6.22840257	-4.00960164	-0.00002745
C	1.89105547	-8.29987363	0.00001782
H	2.57082663	-9.14328316	0.00003954
C	5.36722221	-2.90012416	-0.00002188
H	4.29696824	-3.06652350	-0.00003441
C	7.61738267	-3.80279956	-0.00001215
H	8.27610833	-4.66282255	-0.00001665
C	1.54676830	-5.89989558	-0.00010868
H	1.96178412	-4.89945959	-0.00018254
N	-6.54948192	6.41262668	0.00050442

N	-4.67924713	7.88125072	0.00037565
N	-4.34651278	5.53245458	0.00016170
C	-5.98659111	7.62095488	0.00053814
C	-3.88556362	6.79195406	0.00016220
C	-2.42083663	6.99936545	0.00003214
C	-5.67945891	5.38331349	0.00038362
C	-6.22840363	4.00960376	0.00020671
C	-1.89105640	8.29987458	0.00002735
H	-2.57082656	9.14328495	0.00011511
C	-5.36722221	2.90012714	0.00009387
H	-4.29696830	3.06652771	0.00012766
C	-7.61738352	3.80280049	0.00015867
H	-8.27611013	4.66282266	0.00024945
C	-1.54677158	5.89989616	-0.00008750
H	-1.96178886	4.89946070	-0.00009562
N	-6.96563649	-0.99752880	-0.00017013
N	-8.82880804	-2.46575541	-0.00038848
N	-9.16626379	-0.11171133	-0.00037888
N	-4.48577682	-7.99315281	0.00029831
N	-2.61855598	-6.53008710	0.00005098
N	-2.27853516	-8.87787330	0.00024418
C	-7.50243908	-2.22662693	-0.00023328
C	-6.58683088	-3.38846498	-0.00013224
C	-9.59401189	-1.37423368	-0.00053020
C	-7.82604917	0.03125607	-0.00025466
C	-7.27328003	1.40348004	-0.00009616
C	-3.93972335	-6.76095062	0.00018086
C	-4.85192512	-5.59642174	0.00006698
C	-1.82257990	-7.60956445	0.00009027
C	-0.35852333	-7.39756530	0.00003109
C	-3.60640083	-8.99493091	0.00031774

C	-5.19540367	-3.19724689	-0.00005522
H	-4.80408808	-2.18728916	-0.00006421
C	-8.13452188	2.51263868	0.00000435
H	-9.20484991	2.34556277	-0.00004165
C	-6.24308512	-5.78783240	-0.00000481
H	-6.63390136	-6.79814866	0.00003089
C	0.17154793	-6.09690848	-0.00006202
H	-0.50761913	-5.25324226	-0.00010034
C	-4.33703277	-4.28963798	0.00003522
H	-3.26314470	-4.14838091	0.00008991
C	0.51519608	-8.49696977	0.00007080
H	0.09944984	-9.49728257	0.00013847
C	-7.10185941	-4.69492601	-0.00010864
H	-8.17599498	-4.83553746	-0.00016749
C	-5.88410900	1.61060466	-0.00004515
H	-5.22487472	0.75120322	-0.00011498
H	4.01120944	10.00459893	-0.00009770
H	10.67081663	1.52860821	0.00017619
H	6.65836512	-8.47653210	0.00000167
H	-6.65836781	8.47653432	0.00061492
H	-10.67081197	-1.52861125	-0.00043668
H	-4.01120929	-10.00460242	0.00045718

### STCH-CTF<sub>10</sub> (molecular fragment)

Charge = 0

Multiplicity = 1

N	-7.01947631	-5.92756805	0.00000000
N	-4.80736666	-5.07679079	0.00000000
N	-5.15891021	-7.42013815	0.00000000
N	-7.01494067	1.49120988	0.00000000
N	-9.29018324	0.83063242	0.00000000

N	-8.71197311	3.14343542	0.00000000
C	-6.13428506	-4.91202413	0.00000000
C	-6.63725698	-3.51934392	0.00000000
C	-4.34950530	-6.33854319	0.00000000
C	-2.89235235	-6.52969789	0.00000000
C	-6.46255874	-7.14250388	0.00000000
C	-7.97166102	0.55241729	0.00000000
C	-7.53149154	-0.85818717	0.00000000
C	-9.58399208	2.13258412	0.00000000
C	-7.41797736	2.76715004	0.00000000
C	-6.36787020	3.80966987	0.00000000
C	-8.01198501	-3.23543468	0.00000000
H	-8.71824444	-4.05753894	0.00000000
C	-2.03945864	-5.41024178	0.00000000
H	-2.47820714	-4.42031026	0.00000000
C	-6.15678255	-1.14626014	0.00000000
H	-5.44942678	-0.32698302	0.00000000
C	-6.70236239	5.17279531	0.00000000
H	-7.74785402	5.45791647	0.00000000
C	-8.45598076	-1.91502835	0.00000000
H	-9.51565868	-1.68754494	0.00000000
C	-5.01449031	3.43257105	0.00000000
H	-4.76441673	2.37924635	0.00000000
C	-5.71580238	-2.45976592	0.00000000
H	-4.65769784	-2.68759748	0.00000000
C	-2.32349533	-7.81342792	0.00000000
H	-2.97749567	-8.67787753	0.00000000
N	-3.64317769	8.08019501	0.00000000
N	-1.33142906	8.63627753	0.00000000
N	-2.00551808	6.36260012	0.00000000
C	-2.62811716	8.94435469	0.00000000

C	-1.06285558	7.31508202	0.00000000
C	0.35793173	6.89897391	0.00000000
C	-3.28074765	6.78246030	0.00000000
C	-4.34894325	5.76037879	0.00000000
C	1.37028234	7.87168933	0.00000000
H	1.09205392	8.91848511	0.00000000
C	-4.01618498	4.39634911	0.00000000
H	-2.97170102	4.11022959	0.00000000
C	-5.70161011	6.13938728	0.00000000
H	-5.95128461	7.19362034	0.00000000
C	0.71161332	5.53920783	0.00000000
H	-0.07321457	4.79247981	0.00000000
C	-0.10744155	-6.85069469	0.00000000
C	4.11047608	-8.06122337	0.00000000
C	4.98600134	-6.92812015	0.00000000
C	-0.94162591	-7.97787203	0.00000000
H	-0.50633254	-8.97343811	0.00000000
C	4.44090625	-5.63119710	0.00000000
H	3.36344884	-5.50852053	0.00000000
C	6.37791858	-7.11715126	0.00000000
H	6.78653502	-8.12154852	0.00000000
C	-0.66267078	-5.56417733	0.00000000
H	0.00000000	-4.70545942	0.00000000
N	7.08377478	-2.31356786	0.00000000
N	9.30328651	-1.47187579	0.00000000
N	8.92541591	-3.81377571	0.00000000
N	7.10291062	5.11301291	0.00000000
N	4.82211888	4.45213154	0.00000000
N	5.39330483	6.75765660	0.00000000
C	7.96563200	-1.29907482	0.00000000
C	7.46540053	0.09292703	0.00000000

C	9.71198148	-2.73770499	0.00000000
C	7.60562240	-3.54909169	0.00000000
C	6.68578316	-4.71264104	0.00000000
C	6.13527298	4.17457226	0.00000000
C	6.57368839	2.75917414	0.00000000
C	4.49215727	5.75505426	0.00000000
C	3.06187331	6.13415176	0.00000000
C	6.66698203	6.37109749	0.00000000
C	6.09026863	0.38139023	0.00000000
H	5.37952796	-0.43660688	0.00000000
C	7.21882193	-6.01226081	0.00000000
H	8.29432753	-6.13747039	0.00000000
C	7.94778851	2.46795939	0.00000000
H	8.65641347	3.28658195	0.00000000
C	2.05013407	5.16014529	0.00000000
H	2.32731621	4.11264228	0.00000000
C	5.64869709	1.70209328	0.00000000
H	4.58920772	1.92966639	0.00000000
C	2.70639507	7.49357356	0.00000000
H	3.49073469	8.24015619	0.00000000
C	8.38811743	1.15232874	0.00000000
H	9.44689940	0.92585272	0.00000000
C	5.29396117	-4.53236265	0.00000000
H	4.89388256	-3.52563182	0.00000000
H	-7.14334876	-7.99114120	0.00000000
H	-10.63924517	2.39644304	0.00000000
H	-2.88245505	10.00199834	0.00000000
H	10.78577530	-2.91105068	0.00000000
H	7.42119931	7.15503210	0.00000000
N	3.37165613	-8.96084491	0.00000000
O	1.24864562	-6.93570707	0.00000000

H 1.55843469 -7.85715029 0.00000000

## References

- 1 Y. Gao, Y. Zhu, L. Lyu, Q. Zeng, X. Xing and C. Hu, *Environ. Sci. Technol.*, 2018, **52**, 14371–14380.
- 2 X. Wang and T. Lim, *Applied Catal. B, Environ.*, 2010, **100**, 355–364.
- 3 H. Li, C. Shan and B. Pan, *Environ. Sci. Technol.*, 2018, **52**, 2197–2205.
- 4 G. Zhang and X. Wang, *J. Catal.*, 2013, **307**, 246–253.
- 5 S. Huang, Y. Zhang, C. Du and Y. Su, *Chem. Commun.*, 2020, **56**, 6054–6057.
- 6 G. D. Fang, D. D. Dionysiou, S. R. Al-Abed and D. M. Zhou, *Appl. Catal. B Environ.*, 2013, **129**, 325–332.
- 7 W. Qin, G. Fang, Y. Wang and D. Zhou, *Chem. Eng. J.*, 2018, **348**, 526–534.
- 8 X. Hu, H. Ji, F. Chang and Y. Luo, *Catal. Today*, 2014, **224**, 34–40.
- 9 H. Wang, Q. Li, S. Zhang, Z. Chen, W. Wang, G. Zhao, L. Zhuang, B. Hu and X. Wang, *Catal. Today*, 2019, **335**, 110–116.
- 10 M. Wang, Y. Zeng, G. Dong and C. Wang, *Chinese J. Catal.*, 2020, **41**, 1498–1510.
- 11 D. Chen, J. Liu, Z. Jia, J. Fang, F. Yang and Y. Tang, *J. Hazard. Mater.*, 2019, **361**, 294–304.
- 12 Y. Deng, L. Tang, G. Zeng, Z. Zhu, M. Yan, Y. Zhou, J. Wang, Y. Liu and J. Wang, *Appl. Catal. B Environ.*, 2017, **203**, 343–354.
- 13 D. Xiao, K. Dai, Y. Qu, Y. Yin and H. Chen, *Appl. Surf. Sci.*, 2015, **358**, 181–187.